JOURNAL OF ENZYME INHIBITION AND MEDICINAL CHEMISTRY
2021, VOL. 36, NO. 1, 549–560
https://doi.org/10.1080/14756366.2020.1759582

Taylor & Francis
Taylor & Francis Group

RESEARCH PAPER

OPEN ACCESS Check for updates

Design, synthesis and biological evaluation of 1-Aryl-5-(4-arylpiperazine-1-carbonyl)-1*H*-tetrazols as novel microtubule destabilizers

Chao Wang[a], Yuelin Li[a], Zi Liu[b], Zeyu Wang[c], Zihan Liu[a], Shuai Man[b], Yujing Zhang[a], Kai Bao[c], Yingliang Wu[b], Qi Guan[a], Daiying Zuo[b] and Weige Zhang[a]

[a]Key Laboratory of Structure-Based Drug Design and Discovery, Ministry of Education, Shenyang Pharmaceutical University, Shenyang, China; [b]Department of Pharmacology, Shenyang Pharmaceutical University, Shenyang, China; [c]Wuya College of Innovation, Shenyang Pharmaceutical University, Shenyang, China

ABSTRACT

A series of 1-aryl-5-(4-arylpiperazine-1-carbonyl)-1*H*-tetrazols as microtubule destabilizers were designed, synthesised and evaluated for anticancer activity. Based on bioisosterism, we introduced the tetrazole moiety containing the hydrogen-bond acceptors as B-ring of XRP44X analogues. The key intermediates ethyl 1-aryl-1*H*-tetrazole-5-carboxylates **10** can be simply and efficiently prepared *via* a microwave-assisted continuous operation process. Among the compounds synthesised, compound **6–31** showed noteworthy potency against SGC-7901, A549 and HeLa cell lines. In mechanism studies, compound **6–31** inhibited tubulin polymerisation and disorganised microtubule in SGC-7901 cells by binding to tubulin. Moreover, compound **6–31** arrested SGC-7901cells in G2/M phase. This study provided a new perspective for development of antitumor agents that target tubulin.

ARTICLE HISTORY
Received 9 February 2020
Revised 6 April 2020
Accepted 18 April 2020

KEYWORDS
Tetrazole; microwave; antiproliferative activity; microtubule destabilizer; molecular docking

1. Introduction

Microtubule, is considered an important target for anticancer drug discovery, playing a crucial role in a wide range of fundamental cell functions including the shape maintenance, intracellular transport and cell division[1]. Microtubule-targeted agents, according to the mechanism of interfering with microtubule dynamics, have been classified into microtubule stabilisers (taxanes and epothilones) and microtubule destabilizers (alkaloids and colchicine (**1**))[2]. Given the extensively successful clinical use of vinca alkaloids, the microtubule destabilizers have aroused great interest among medicinal chemists[3]. Over the past decades, a great many outstanding microtubule destabilizers have been reported, such as combretastatin A-4 (CA-4, **2**)[4] and XRP44X (**3**)[5] (Figure 1).

XRP44X, an arylpyrazole derivative, was developed by Wasylyk et al. as a novel microtubule destabilizer, which prominently inhibited the polymerisation process of tubulin into microtubules by interacting with the colchicine-binding site of tubulin and displayed potent cytotoxic activities against a wide variety of human cancer cell lines at low nanomolar concentrations. A series of aryloxazole derivatives have been synthesised and were found to be potent inhibitors of tubulin polymerisation by Pae and co-workers. Among them, compound **4** showed excellent antiproliferative *in vitro* and effectively reduced tumour growth *in vivo* using a tumour xenograft model[6]. Our groups discovered a series of aryltriazole derivatives as a result of structural modifications of the lead compound XRP44X[7]. The most potent compound 5 exhibited excellent antiproliferative activity *via* disrupting cytoskeleton.

As shown in Figure 1, XRP44X and its analogues molecules can be divided into three major structural elements i.e., A-ring (substituted phenyl), B-ring (five-membered heterocycle, such as pyrazole, oxazole and 1,2,3-triazole), C-ring (piperazine), D-ring (substituted phenyl), and a carbonyl linkage between B-ring and C-ring. Bioisosterism plays a major role in the search for analogues of an active drug molecule. Application of bioisosterism instead of the B-ring on the structure of XRP44X is one of the strategies often used in design of the XRP44X analogues[6]. The modification of B-ring has led to varied cytotoxic activity.

In the last decade, there has been great interest in compounds containing the 1*H*-tetrazol scaffold because of its unique chemical structure and broad spectrum of biological properties including anticancer activity. For example, the 1-(3,4,5-Trimethoxyphenyl)-5-(4-ethoxyphenyl)-1*H*-tetrazole was designed as tubulin inhibitor, which showed low IC_{50} values at nanomolar level[8].

As a part of our continuing effort on the development of novel antitumor agents, we designed a series of novel XRP44X analogues by introducing an 1*H*-tetrazol, hydrogen-bonding acceptors, as B-ring of XRP44X (Figure 2). Herein, we described the detailed synthetic routes, antiproliferative, tubulin polymerisation, analysis of immunofluorescence staining and cell cycle analysis of these compounds.

2. Result and discussion

2.1. Chemistry

The general synthetic approach for the preparation of 1-aryl-5-(4-arylpiperazine-1-carbonyl)-1*H*-tetrazol (**6**) was illustrated in Scheme 1. First of all, the substituted aromatic amines (**7**) were

CONTACT Qi Guan guanqi@syphu.edu.cn; Weige Zhang zhangweige2000@sina.com Key Laboratory of Structure-Based Drug Design and Discovery, Ministry of Education, Shenyang Pharmaceutical University, Shenyang, China; Daiying Zuo zuodaiying@163.com Department of Pharmacology, Shenyang Pharmaceutical University, Shenyang, China

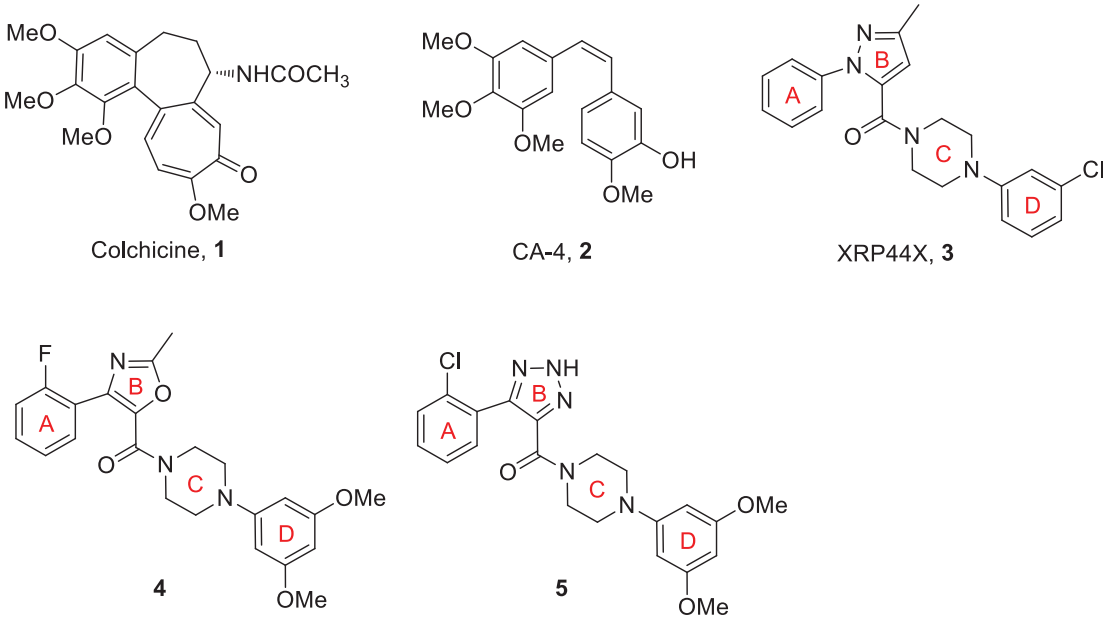

Figure 1. Chemical structures of some microtubule destabilizers.

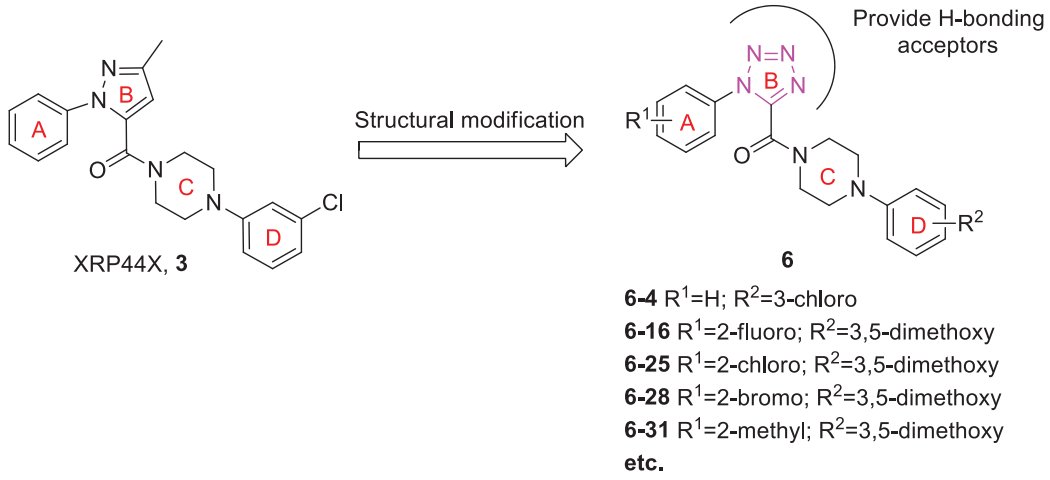

Figure 2. Design of the target compounds.

reacted with ethyl oxalate in dichloromethane to afford corresponding intermediates (**8**) at room temperature[9,10]. Subsequently, **8** were reacted with triphenylphosphine and carbon tetrachloride to give corresponding (*E*)-ethyl 2-chloro-2-(arylimino)acetates (**9**) *via* Appel reaction under microwave irradiation. Without further purification, compounds **9** reacted with sodium azide in acetonitrile to get the key intermediates ethyl 1-aryl-1*H*-tetrazole-5-carboxylates (**10**) in a continuous operation process[11–13]. Finally, the key intermediates **10** reacted with corresponding arylpiperazines to afford the target compounds (**6**) in the presence of trimethylaluminium[14].

Under conventional heating conduction, the reaction of **8** with PPh_3 in CCl_4 to generate (*E*)-ethyl 2-chloro-2-(arylimino)acetates (**9**) suffered from long reaction time and low yields (Table 1, entries 1–5). Microwave irradiation offered many advantages, such as rate enhancements and higher yields, over conventional heating and had become a popular technique that was widely used in organic synthesis today[15–18]. When microwave irradiation was incorporated into synthesis of **9**–**8**, we found that the reaction rate was greatly improved. We systematically screened the influence of reaction temperature and time on the yield of **9**–**8** under microwave conditions. As shown in Table 1, the optimised condition was confirmed to be microwave irradiation at 130 °C for 20 min (entry 8). Accordingly, all intermediates **9** were obtained smoothly.

2.2. Biological evaluation

2.2.1. In vitro *antiproliferative activity*

All the target compounds have been evaluated for *in vitro* the antiproliferative activities against different three human cancer cell lines (gastric adenocarcinoma SGC-7901 cells, lung adenocarcinoma A549 cells and cervical carcinoma HeLa cells) using MTT assay with colchicine and CA-4 as references. To examine the more detailed structure-activity relationships, modifications towards A-ring and D-ring were performed.

Careful observation of Table 2 revealed that introduction of substituent into the ortho-position of A-ring could remarkably enhance the antiproliferative effect, such as **6**–**28** ∼ **6**–**30**. The overall preference order of substituent at the ortho-position of A-ring is as follows: 2-methyl > 2-fluoro > 2-chloro > H. Furthermore, in the case of D-ring 3,5-dimethoxyphenyl fused

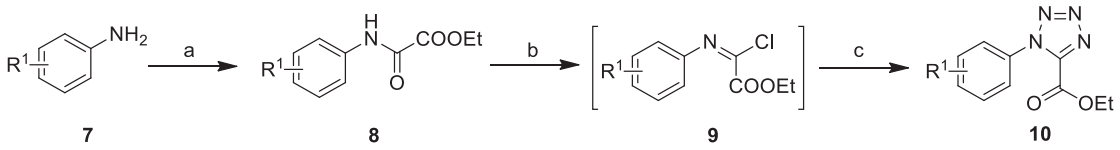

	R^1
7-1~10-1	H
7-2~10-2	2-fluoro
7-3~10-3	3-fluoro
7-4~10-4	4-fluoro
7-5~10-5	2-chloro
7-6~10-6	3-chloro
7-7~10-7	2-bromo
7-8~10-8	3-bromo
7-9~10-9	4-bromo
7-10~10-10	2-methyl
7-11~10-11	3-methyl

	R^1	R^2		R^1	R^2
6-1	H	H	**6-17**	3-fluoro	3-methoxy
6-2	H	3-fluoro	**6-18**	3-fluoro	3,5-dimethoxy
6-3	H	2-chloro	**6-19**	4-fluoro	3-methoxy
6-4	H	3-chloro	**6-20**	4-fluoro	3,5-dimethoxy
6-5	H	3-methyl	**6-21**	2-chloro	3-methyl
6-6	H	3-methoxy	**6-22**	2-chloro	3-methoxy
6-7	H	4-methoxy	**6-23**	2-chloro	4-methoxy
6-8	H	3-trifluoromethyl	**6-24**	2-chloro	3,4-dimethyl
6-9	H	3,4-dimethyl	**6-25**	2-chloro	3,5-dimethoxy
6-10	H	2,6-dimethyl	**6-26**	3-chloro	3-methoxy
6-11	H	3,4-dimethoxy	**6-27**	3-chloro	3,5-dimethoxy
6-12	H	2,5-dimethoxy	**6-28**	2-bromo	3,5-dimethoxy
6-13	H	3,5-dimethoxy	**6-29**	3-bromo	3,5-dimethoxy
6-14	2-fluoro	3-methyl	**6-30**	4-bromo	3,5-dimethoxy
6-15	2-fluoro	3-methoxy	**6-31**	2-methyl	3,5-dimethoxy
6-16	2-fluoro	3,5-dimethoxy	**6-32**	3-methyl	3,5-dimethoxy

Scheme 1. Reagents and conditions: (a) EtO_2CCOCl, Et_3N, DCM, rt., 1 h; (b) Ph_3P, CCl_4, 130 °C, MW, 20 min; (c) NaN_3, MeCN, rt., overnight; (d) arylpiperazines, $AlMe_3$ (1.0 M solution in heptane), DCM, rt., overnight.

Table 1. The optimisation of conditions for the preparation of compound **9–8**.

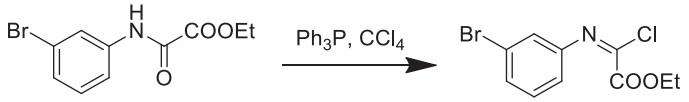

8-8 **9-8**

Entry	Heating	Temp (°C)	Time (min)	Yield (%)
1[a]	Oil bath	Reflux	60	Trace
2[a]	Oil bath	Reflux	360	10[c]
3[a]	Oil bath	Reflux	600	30[c]
4[a]	Oil bath	Reflux	720	41[c]
5[a]	Oil bath	Reflux	960	52[d]
6[b]	MW	120	20	45[c]
7[b]	MW	130	10	50[d]
8[b]	**MW**	**130**	**20**	**67**[d]
9[b]	MW	130	30	62[d]
10[b]	MW	140	20	60[d]

[a]Reaction conditions: ethyl 2-((3-bromophenyl)amino)-2-oxoacetate (1 mmol), Ph3P (1.5 mmol), CCl4 (5 ml).
[b]Reaction conditions: ethyl 2-((3-bromophenyl)amino)-2-oxoacetate (1 mmol), Ph3P (1.5 mmol), CCl4 (5 ml), MW.
[c]The yields were determined by HPLC.
[d]Isolated yields.

compounds showed significant anticancer activities. Compound **6–31** was found to be the most potent compound among all the target compounds with IC50 value of 0.090–0.650 μM against the three cancer cell lines.

2.2.2. Effect on tubulin polymerisation

In order to examine whether the compounds interact with tubulin, we chose the most active compound **6–31** to evaluate for its inhibition of tubulin polymerisation *in vitro*. Microtubule polymerisation inhibitor (CA-4) and microtubule stabilising agent (Paclitaxel) were used as the positive and negative controls, respectively. As shown in Figure 3, compound **6–31** inhibited tubulin assembly in a concentration-dependent manner. In contrast, paclitaxel could raise the proportion of tubulin polymerisation in comparison with the untreated cells. The results suggested that compound **6–31** interferes with the microtubule polymerisation in a similar way as CA-4.

2.2.3. Analysis of immunofluorescence staining

To further confirm the influence of inhibition of tubulin polymerisation in cells, immunofluorescence staining was carried out. SGC-7901 cell lines were treated for 24 h with CA-4 and compound **6–31**, at their respective 2-fold IC_{50} concentrations. As given in Figure 4, the microtubule network without drug treatment displays normal arrangement and organisation in control cells. Whereas SGC-7901 cells were treated with CA-4 and compound **6–31** and the results demonstrated that microtubules were destroyed and wrapped around the nucleus in comparison with the control. These results suggest that compound **6–31** inhibits microtubule assembly and disrupts cytoskeleton similarly to CA-4.

2.2.4. Cell cycle analysis

It is well known that most tubulin inhibitors induce cell cycle arrest in the G2/M phase[7]. Thus, the effect of compound **6–31**on the cell cycle of SGC-7901 cells was analysed by flow cytometry. SGC-7901 cells were incubated with CA-4 or compound **6–31**, at their respective two-fold IC_{50} concentrations, and the proportion of tested cells at different cell cycle phases was analysed by flow cytometry after 0, 12, 24, 36, 48, and 72 h of treatment, respectively.

Table 2. The antiproliferative activities of all target compounds

Compound	R^1	R^2	(IC_{50} ± SD, μM)[a] SGC-7901	A549	HeLa
6–1	H	H	>30	9.92 ± 0.46	>30
6–2	H	3-fluoro	28.3 ± 2.1	>30	>30
6–3	H	2-chloro	>30	>30	>30
6–4	H	3-chloro	13.8 ± 0.8	8.22 ± 0.23	18.2 ± 1.8
6–5	H	3-methyl	27.8 ± 2.0	25.3 ± 1.9	22.1 ± 1.6
6–6	H	3-methoxy	15.5 ± 1.2	13.2 ± 1.0	19.3 ± 1.7
6–7	H	4-methoxy	>30	>30	>30
6–8	H	3-trifluoromethyl	16.1 ± 1.4	15.0 ± 1.2	20.6 ± 1.8
6–9	H	3,4-dimethyl	>30	>30	>30
6–10	H	2,6-dimethyl	>30	>30	>30
6–11	H	3,4-dimethoxy	>30	27.3 ± 1.9	>30
6–12	H	2,5-dimethoxy	2.47 ± 0.21	3.86 ± 0.27	3.34 ± 0.23
6–13	H	3,5-dimethoxy	1.68 ± 0.12	3.10 ± 0.25	3.11 ± 0.19
6–14	2-fluoro	3-methyl	17.2 ± 1.4	5.80 ± 0.30	>30
6–15	2-fluoro	3-methoxy	11.3 ± 0.9	10.0 ± 1.1	26.1 ± 2.3
6–16	2-fluoro	3,5-dimethoxy	0.504 ± 0.021	2.17 ± 0.20	0.360 ± 0.017
6–17	3-fluoro	3-methoxy	29.8 ± 3.0	20.9 ± 1.5	28.7 ± 3.2
6–18	3-fluoro	3,5-dimethoxy	4.2 ± 0.24	6.71 ± 0.19	1.01 ± 0.05
6–19	4-fluoro	3-methoxy	>30	>30	27.6 ± 2.7
6–20	4-fluoro	3,5-dimethoxy	12.2 ± 1.6	>30	10.5 ± 0.9
6–21	2-chloro	3-methyl	4.59 ± 0.18	10.5 ± 0.41	10.6 ± 0.47
6–22	2-chloro	3-methoxy	11.8 ± 0.50	11.7 ± 0.49	>30
6–23	2-chloro	4-methoxy	>30	>30	>30
6–24	2-chloro	3,4-dimethyl	24.3 ± 1.6	>30	22.0 ± 1.5
6–25	2-chloro	3,5-dimethoxy	1.08 ± 0.13	3.12 ± 0.15	0.580 ± 0.023
6–26	3-chloro	3-methoxy	>30	>30	29.4 ± 0.6
6–27	3-chloro	3,5-dimethoxy	1.51 ± 0.09	7.77 ± 0.17	1.85 ± 0.13
6–28	2-bromo	3,5-dimethoxy	2.53 ± 0.11	>30	5.67 ± 0.19
6–29	3-bromo	3,5-dimethoxy	4.73 ± 0.14	>30	7.48 ± 0.18
6–30	4-bromo	3,5-dimethoxy	>30	29.4 ± 3.1	>30
6–31	2-methyl	3,5-dimethoxy	**0.090 ± 0.008**	**0.650 ± 0.017**	**0.268 ± 0.012**
6–32	3-methyl	3,5-dimethoxy	1.44 ± 0.09	2.34 ± 0.16	0.812 ± 0.034
CA–4[b]			0.036 ± 0.002	0.070 ± 0.007	0.034 ± 0.004
Colchicine[b]			0.096 ± 0.009	0.075 ± 0.011	0.066 ± 0.005

[a]IC_{50}: the half maximal inhibitory concentration.
[b]Used as positive controls.

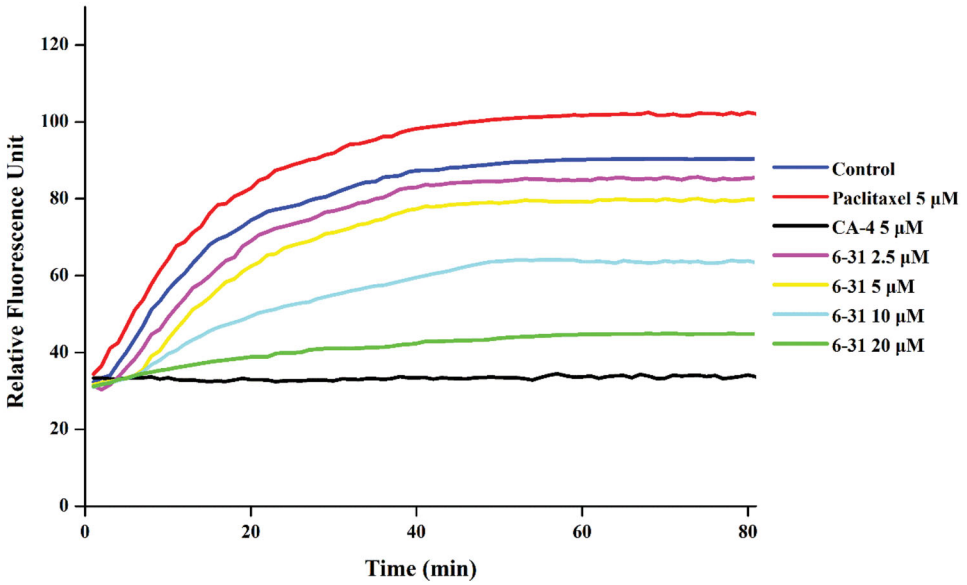

Figure 3. The effect of compound **6–31** on tubulin polymerisation. The tubulin had been pre-incubated for 1 min with **6–31** at 2.5 μM, 5 μM, 10 μM and 20 μM, CA-4 at 5 μM, Paclitaxel at 5 μM or vehicle DMSO at room temperature before GTP was added to start the tubulin polymerisation reactions. The reaction was monitored at 37 °C.

As shown in Figure 5, cells treated with either CA-4 or compound **6–31** were arrested at the G2/M phase. In addition, whereas CA-4 or **6–31** induced a sharply decrease of G1 cell population, and an increase of G2/M cell population in time-dependent manner. After treatment with compound **6–31** for 12 h, the percentage of cells in the G2/M phase increased to 63.0% from 22.2%. After 72 h, there were significantly increased numbers of cells in sub-G1 after exposure to CA-4 and compound

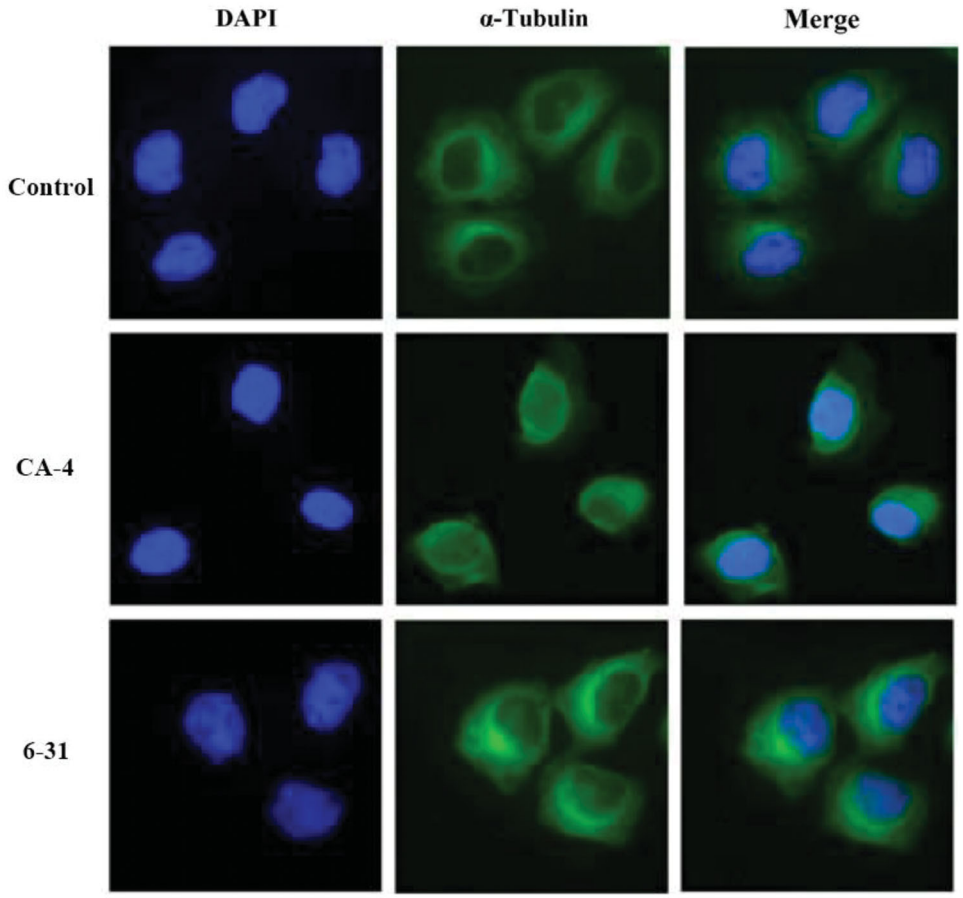

Figure 4. Effects of **6**–**31** and CA-4, at their respective two-fold IC_{50} concentrations, on the cellular microtubule network and microtubule reassemble by immunofluorescence. SGC-7901 cells were treated with **6**–**31** or CA-4 for 24 h, and then direct microscopy detection of the fixed and stained cell was performed. The cellular microtubules were stained with anti-a-tubulin-FITC specific antibodies (green). DNA was stained by 4,6-diamidino-2-phenylindole (DAPI, blue). (For interpretation of the references to colour in this figure legend, the reader is referred to the Web version of this article).

6–31, respectively, indicating the induction of apoptosis. The cell cycle analysis suggests that compound **6–31** arrests SGC-7901 cell in G2/M phase followed by cellular apoptosis.

2.3. Molecular modelling

To further understand the binding interactions, molecular docking of the most active compound **6–31** was carried out with tubulin crystal structure (PDB code: 3HKC) using the CDOCKER programme of Discovery Studio 3.0 software. As shown in Figure 6, XRP44X and compound **6–31** are located at the same position with a similar conformation in the binding pocket. Meanwhile, the hydrogen bond exists between the carbonyl group of XRP44X or compound **6–31** with amino acid residue Alaβ317. Moreover, it is worth noting that the residue of Asnβ258 forms a hydrogen bond with the 2*N* of 1*H*-tetrazole of compound **6–31** and the residue of Lysβ352 forms a hydrogen bond with the 4*N* of 1*H*-tetrazole of compound **6–31**. It suggests that the 1*H*-tetrazole derivatives can not only maintain the right conformation, but also nicely nestle in the active site. The 1*H*-tetrazole moiety and unique active site interactions set the stage for structure-based design of more potent derivatives.

2.4. Prediction of drug-like properties

Furthermore, to explore the drug-like properties of the target compounds, some physicochemical properties of XRP44X and compound **6–31** were predicted using free online website (http://www.swissadme.ch/index.php) for their adaptability with Lipinski's rule of five[19]. As shown in Table 3, XRP44X and compound **6–31** conform well to the Lipinski's rule of five. Compared with XRP44X, compound **6–31** has a lower value of lipid-water partition coefficient. This data indicates that compound **6–31** may have better water solubility than XRP44X. In addition, compound **6–31** exists six hydrogen bond receptors, much more than XRP44X, which helps to reduce the binding energy between the compound and the action site.

3. Conclusion

In summary, we had designed and synthesised a series of XRP44X derivatives having a 1*H*-tetrazole B-ring as the hydrogen-bonding acceptors and found that these compounds showed good growth inhibition activities against a range of human cancer cells. Among them, compound **6–31**, represented the most active compound with IC_{50} values of 0.090–0.650 μM against three cancer cell lines. Moreover, compound **6–31** could disrupt microtubule network in living cancer cells, arrest cell cycle at G2/M phase and induce apoptosis in a dose- and time-dependent manner. Docking studies suggest that compound **6–31** may be a potential tubulin inhibitor. A hydrogen bond was present between Alaβ317 with the carbonyl group of compound **6–31**. Another two hydrogen bonds were also observed between Asnβ258 and Lysβ352 with the 1*H*-tetrazole (B-ring). In addition, the prediction of drug-like properties studies shows that compound **6–31** has better pharmacokinetic properties than XRP44X. All of these results indicate compound

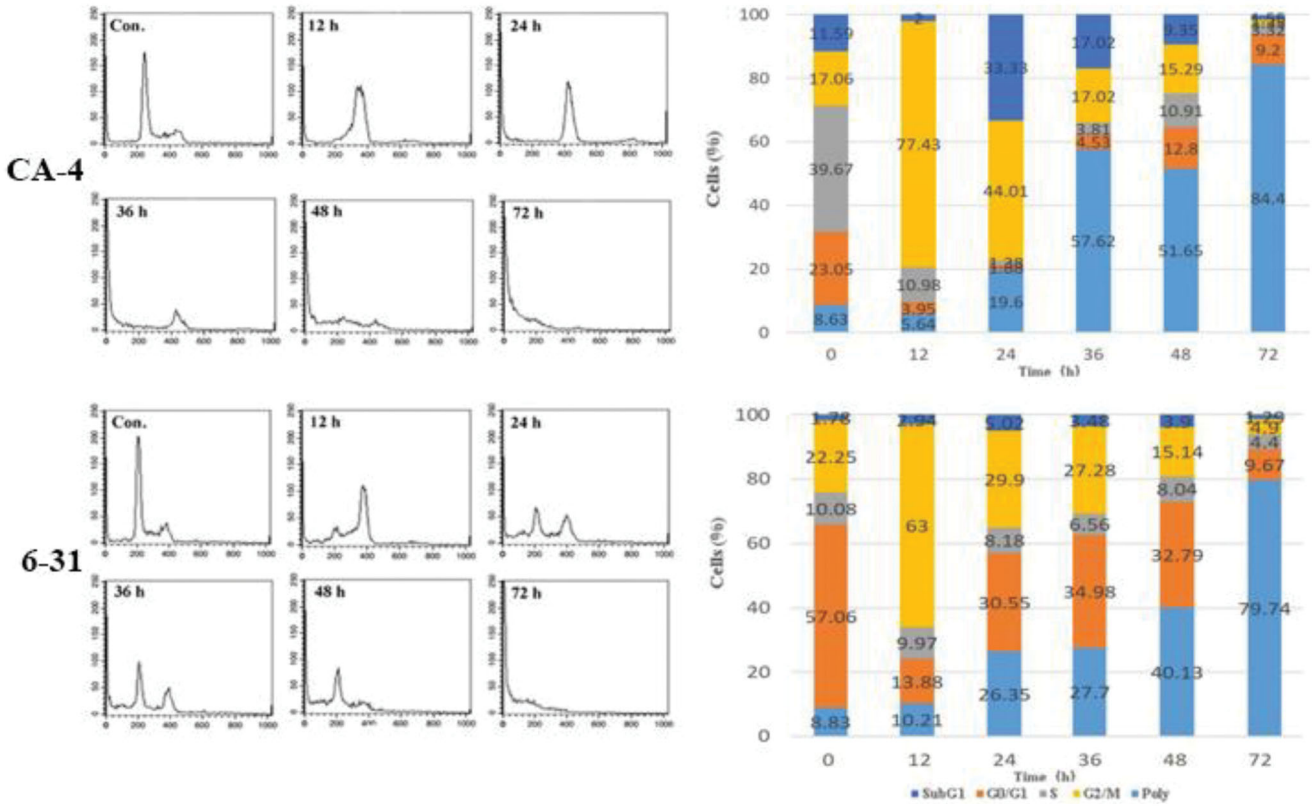

Figure 5. The effect of CA-4 and compound **6–31** on cell cycle. SGC-7901 cells lines treated with CA-4 and compound **6–31**, at their respective two-fold IC_{50} concentrations, for 0, 12, 24, 36, 48 and 72 h.

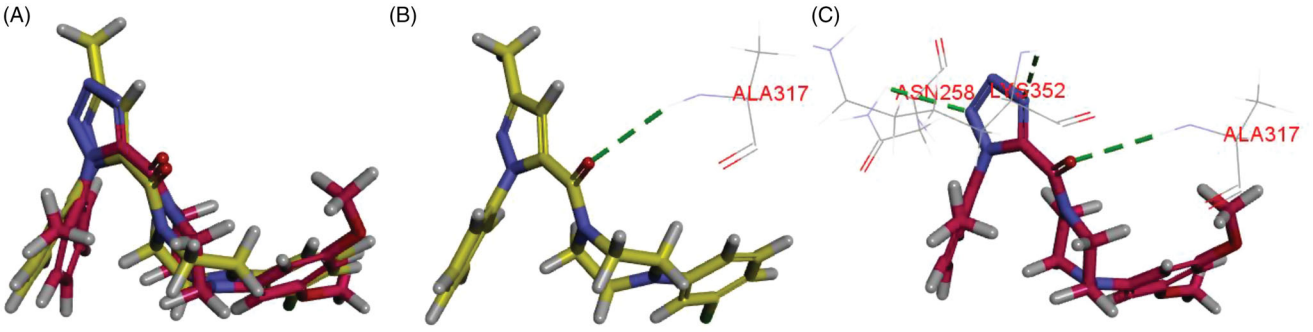

Figure 6. (A) Superimposition of XRP44X (yellow) and **6–31** (red) in colchicine-binding site; (B) interaction of XRP44X (yellow) with tubulin (green dotted lines represent H-bond); (C) Interactions of **6–31** (red) with tubulin (green dotted lines represent H-bond).

Table 3. Prediction of physicochemical properties[a] of **3** and **6–31.**

Compound	miLogP	TPSA	natoms	MW	nON	nOHNH	nrotb
Standard	<5	<140		<500	<10	<5	≤10
3	3.48	41.37	48	380.87	2	0	4
6–31	2.29	85.61	54	408.45	6	0	6

[a]miLogP: molinspiration predicted Log P; TPSA: topological polar surface area; natoms: No. of atoms; MW: molecular weight; nON: No. of hydrogen bond acceptors; nOHNH: No. of hydrogen bond donors; nrotb: No. of rotatable bonds.

6–31 as a promising microtubule destabilizer for further investigation in anticancer drug development.

4. Experimental

4.1. Chemistry

4.1.1. Materials and methods

All of reagents and solvents were purchased from chemical company. ^{1}H NMR and ^{13}C NMR spectra were tested in $CDCl_3$ with TMS as the internal reference on a Bruker AVANCE 400 or 600 (^{1}H at 400 or 600 MHz, ^{13}C at 150 MHz). Mass spectra (MS) were measured on an Agilent 1100-sl mass spectrometer with an electrospray ionisation source from Agilent Co. Ltd. High resolution accurate mass determinations (HRMS) for all of the final target compounds were obtained on a Bruker Micromass Time of Flight mass spectrometer equipped with electrospray ionisation (ESI). TLC analysis was used for determining the extent of reactions under UV light (wavelength: 365 nm and 254 nm). Melting point was measured (uncorrected) on hot-stage microscope (Beijing Taike, X-4). The microwave reactions were carried out in a single mode cavity microwave synthesiser (CEM Corporation, NC, USA).

4.1.2. General synthetic procedures for arylpiperazines

A solution of arylamine (1 mmol), bis(2- chloroethyl)amine hydrochloride (1.1 mmol) and K_2CO_3 (3 mmol) in *n*-BuOH were stirred at irradiated in a microwave reactor for 30 min at 150 °C. The

reaction mixture was cooled to room temperature and dissolved in methanol (4 ml), followed by the addition of diethyl ether (150 ml). The precipitate formed was recovered by filtration and washed with diethyl ether to obtain arylpiperazine as HCl salt. The HCl salt was used for the next reaction without further purification[20,21].

4.1.3. General synthetic procedures for ethyl 2-oxo-2-(arylamino)acetates (8)

To a solution of substituted aniline (10 mmol) and triethylamine (1 ml, 10 mmol) in DCM was added ethyl chlorooxoacetate (10 mmol) in DCM. The reaction mixture was stirred for 1 h at room temperature. The reaction mixture was poured into water and extracted with DCM (50 ml × 3). The combined organic layer was washed with brine, dried over anhydrous Na_2SO_4, filtered and concentrated to yield the crude product. The crude product was purified by column chromatography (*n*-hexane/EtOAc = 1:2) on silica gel to afford pure products. For example:

4.1.3.1. Ethyl 2-oxo-2-(phenylamino)acetate (8–1). White Solid; yield: 91%; MS (ESI) *m/z* 194.1 $[M+H]^+$.

4.1.3.2. Ethyl 2-((3-bromophenyl)amino)-2-oxoacetate (8–8). White Solid; yield: 92%; MS (ESI) *m/z* 272.0 $[M+H]^+$.

4.1.4. General synthetic procedures for (E)-ethyl 2-chloro-2-(arylimino)acetates (9)

A solution of triphenylphosphine (1.5 mmol) and ethyl 2-oxo-2-(arylamino)acetate (1 mmol) in CCl_4 (5 ml) were stirred at irradiated in a microwave reactor for 20 min at 130 °C. The reaction mixtures were cooled to room temperature and the precipitate was filtered off. The filtrate was concentrated to yield the crude product. The crude product was purified by column chromatography (*n*-hexane/EtOAc = 4:1) on silica gel to afford pure products. For example:

4.1.4.1. (E)-Ethyl 2-((3-bromophenyl)imino)-2-chloroacetate (9–8). Light yellow oil; yield: 67%; ^{1}H NMR (600 MHz, $CDCl_3$): δ = 7.65 (1H, s), 7.63 (1H, d, J = 1.4 Hz), 7.22 (1H, t, J = 2.9 Hz), 7.16 (1H, t, J = 2.0 Hz), 4.40 (2H, q, J = 7.2 Hz), 1.38 (3H, t, J = 7.1 Hz). ESI-MS: *m/z* = 290.5 $[M+H]^+$.

4.1.5. General synthetic procedures for ethyl 1-aryl-1H-tetrazole-5-carboxylates (10)

Because of the instability of intermediates **9**, we described a microwave-assisted continuous operation process method rather than stepwise operation process for the conversion of **8**–**10**. A solution of triphenylphosphine (1.5 mmol) and ethyl 2-oxo-2-(arylamino)acetate **8** (1 mmol) in CCl_4 (5 ml) were stirred at irradiated in a microwave reactor for 20 min at 130 °C. The reaction mixtures were cooled to room temperature and the precipitate was filtered off. The filtrate was evaporated and dissolved in CH_3CN. Sodium azide (1.2 mmol) was added at room temperature under N_2 for 16 h. The solvent was then removed under reduced pressure and extracted with ethyl acetate (50 ml × 3). The combined organic layer was washed with water and brine and then dried over Na_2SO_4, filtered and concentrated to yield the crude product. The crude product was purified by column chromatography (*n*-hexane/EtOAc = 3:1) on silica gel to afford pure products. For example:

4.1.5.1. Ethyl 1-phenyl-1H-tetrazole-5-carboxylate (10–1). Light yellow Solid; yield: 76%; ^{1}H NMR (600 MHz, $CDCl_3$): δ = 7.70 (3H, m), 7.60 (2H, m), 4.55 (2H, q), 1.47 (3H, t, J = 6.8 Hz). ESI-MS: *m/z* = 219.1 $[M+H]^+$.

4.1.5.2. Ethyl 1-(2-fluorophenyl)-1H-tetrazole-5-carboxylate (10–2). Yellow Solid; yield: 66%; ^{1}H NMR (600 MHz, $CDCl_3$): δ = 7.63 (1H, m), 7.57 (1H, m), 7.40 (1H, t, J = 7.2 Hz), 7.34 (1H, m), 4.46 (2H, q), 1.37 (3H, t, J = 6.8 Hz). ESI-MS: *m/z* = 237.1 $[M+H]^+$.

4.1.5.3. Ethyl 1–(3-fluorophenyl)-1H-tetrazole-5-carboxylate (10–3). Light yellow Solid; yield: 71%; ^{1}H NMR (600 MHz, $CDCl_3$): δ = 7.57 (1H, m), 7.34 (2H, m), 7.29 (1H, m), 4.47 (2H, q), 1.40 (3H, t, J = 8.1 Hz). ESI-MS: *m/z* = 237.0 $[M+H]^+$.

4.1.5.4. Ethyl 1-(4-fluorophenyl)-1H-tetrazole-5-carboxylate (10–4). Light yellow Solid; yield: 77%; ^{1}H NMR (600 MHz, $CDCl_3$): δ = 7.51 (2H, m), 7.27 (2H, m), 4.56 (2H, q), 1.40 (3H, t, J = 7.1 Hz). ESI-MS: *m/z* = 237.1 $[M+H]^+$.

4.1.5.5. Ethyl 1-(2-chlorophenyl)-1H-tetrazole-5-carboxylate (10–5). Yellow Solid; yield: 70%; ^{1}H NMR (600 MHz, $CDCl_3$): δ = 7.61 (2H, m), 7.51 (2H, m), 4.42 (2H, q), 1.34 (3H, t, J = 7.1 Hz). ESI-MS: *m/z* = 253.0 $[M+H]^+$.

4.1.5.6. Ethyl 1-(3-chlorophenyl)-1H-tetrazole-5-carboxylate (10–6). Yellow Solid; yield: 73%; ^{1}H NMR (600 MHz, $CDCl_3$): δ = 7.60 (1H, m), 7.54 (2H, m), 7.42 (1H, m), 4.47 (2H, q), 1.40 (3H, t, J = 7.5 Hz). ESI-MS: *m/z* = 253.0 $[M+H]^+$.

4.1.5.7. Ethyl 1-(2-bromophenyl)-1H-tetrazole-5-carboxylate (10–7). Yellow Solid; yield: 76%; ^{1}H NMR (600 MHz, $CDCl_3$): δ = 7.64 (1H, d, J = 7.8 Hz), 7.35 (1H, t, J = 7.4 Hz), 7.11 (1H, d, J = 8.4 Hz), 6.92 (1H, d, J = 7.8 Hz), 4.48 (2H, q), 1.45 (3H, t, J = 7.4 Hz). ESI-MS: *m/z* = 297.0 $[M+H]^+$.

4.1.5.8. Ethyl 1-(3-bromophenyl)-1H-tetrazole-5-carboxylate (10–8). Light yellow Solid; yield: 62%; ^{1}H NMR (600 MHz, $CDCl_3$): δ = 7.76 (1H, m), 7.70 (1H, m), 7.46 (2H, m), 4.47 (2H, q), 1.40 (3H, t, J = 7.4 Hz). ESI-MS: *m/z* = 297.0 $[M+H]^+$.

4.1.5.9. Ethyl 1-(4-bromophenyl)-1H-tetrazole-5-carboxylate (10–9). Light yellow Solid; yield: 69%; ^{1}H NMR (600 MHz, $CDCl_3$): δ = 7.72 (2H, d, J = 8.5 Hz), 7.40 (2H, d, J = 8.5 Hz), 4.46 (2H, q), 1.40 (3H, t, J = 7.81 Hz). ESI-MS: *m/z* = 297.0 $[M+H]^+$.

4.1.5.10. Ethyl 1-(o-tolyl)-1H-tetrazole-5-carboxylate (10–10). Yellow Solid; yield: 67%; ^{1}H NMR (600 MHz, $CDCl_3$): δ = 7.52 (1H, m), 7.42 (1H, d, J = 7.4 Hz), 7.39 (1H, t, J = 7.7 Hz), 7.25 (1H, dd, J = 1.2 Hz, J = 7.7 Hz), 4.40 (2H, q), 2.05 (1H, s), 1.32 (3H, t, J = 6.8 Hz). ESI-MS: *m/z* = 233.1 $[M+H]^+$.

4.1.5.11. Ethyl 1-(m-tolyl)-1H-tetrazole-5-carboxylate (10–11). Yellow Solid; yield: 75%; ^{1}H NMR (600 MHz, $CDCl_3$): δ = 7.45 (1H, t, J = 8.4 Hz), 7.41 (1H, d, J = 8.1 Hz), 7.28 (2H, t, J = 11.8 Hz), 4.45 (2H, q), 2.46 (3H, s), 1.37 (3H, t, J = 7.3 Hz). ESI-MS: *m/z* = 233.1 $[M+H]^+$.

4.1.6. General synthetic procedures for 1-aryl-5–(4-arylpiperazine-1-carbonyl)-1H-tetrazols (6)

To a solution of arylpiperazine (0.1 mmol) in anhydrous DCM was added trimethylaluminum (0.5 ml, 1 M in heptane). The reaction

was stirred at room temperature under N_2 for 15 min. A solution of an appropriate ethyl 1-aryl-1*H*-tetrazole-5-carboxylate (0.1 mmol) in anhydrous DCM was added and the reaction was stirred at room temperature under N_2 for 16 h. The reaction was quenched with 5 ml of 1 M HCl and diluted with DCM. The combined organic layer was washed with water and brine and then dried over Na_2SO_4, filtered and concentrated to yield the crude product. The crude product was purified by column chromatography (*n*-hexane/EtOAc = 1:1) on silica gel to afford pure products.

4.1.6.1. 1-Phenyl-5–(4-phenylpiperazine-1-carbonyl)-1H-tetrazol (6–1).

White Solid; yield: 45%; Mp: 140.0–141.8 °C; ^{1}H NMR (600 MHz, $CDCl_3$): δ = 7.50 (5H, d, J = 10.8 Hz), 7.22 (2H, t, J = 7.6 Hz), 6.85 (3H, m), 3.86 (2H, s), 3.63 (2H, s), 3.17 (2H, s), 3.07 (2H, s). ^{13}C NMR (150 MHz, $CDCl_3$): δ = 154.6, 149.4, 146.6, 132.7, 129.6, 128.8 (2 C), 128.3 (2 C), 122.9 (2 C), 120.1, 115.9 (2 C), 48.9, 48.4, 45.9, 41.5; HRMS calcd for $C_{18}H_{18}N_6NaO$ $[M + Na]^+$ 357.1440, found 357.1477.

4.1.6.2. 1-Phenyl-5-(4-(3-fluorophenyl)piperazine-1-carbonyl)-1H-tetrazol (6–2).

Light yellow Solid; yield: 49%; Mp: 135.9–137.8 °C; ^{1}H NMR (600 MHz, $CDCl_3$): δ = 7.50 (5H, d), 7.14 (1H, q, J = 7.8 Hz), 6.58 (1H, q, J = 8.5 Hz), 6.51 (2H, m,), 3.84 (2H, t, J = 4.7 Hz), 3.64 (2H, t, J = 4.4 Hz), 3.17 (2H, t, J = 5.0 Hz), 3.08 (2H, t, J = 4.7 Hz). ^{13}C NMR (150 MHz, $CDCl_3$): δ = 162.7 (d, J = 237.7 Hz), 154.6, 151.0 (d, J = 9.2 Hz), 146.6, 132.7, 129.7, 129.4 (d, J = 10.2 Hz), 128.8 (2 C), 123.0 (2 C), 110.9 (d, J = 2.5 Hz), 106.2 (d, J = 20.4 Hz), 102.6 (d, J = 24.0 Hz), 48.3, 47.8, 45.7, 41.3; HRMS calcd for $C_{18}H_{17}FN_6NaO$ $[M + Na]^+$ 375.1346, found 375.1378.

4.1.6.3. 1-Phenyl-5-(4-(2-chlorophenyl)piperazine-1-carbonyl)-1H-tetrazol (6–3).

Light yellow Solid; yield: 60%; Mp: 76.7–78.4 °C; ^{1}H NMR (600 MHz, $CDCl_3$): δ = 7.59 (5H, m), 7.01 (4H, m), 3.96 (2H, t, J = 4.2 Hz), 3.68 (2H, t, J = 4.7 Hz), 3.10 (2H, t, J = 5.0 Hz), 3.02 (2H, t, J = 4.9 Hz). ^{13}C NMR (150 MHz, $CDCl_3$): δ = 154.8, 147.0, 146.7, 129.7, 129.7, 128.8 (2 C), 128.6, 126.7, 123.7, 122.87 (2 C), 119.6, 114.3, 50.3, 49.8, 46.4, 41.9; HRMS calcd for $C_{18}H_{17}ClN_6NaO$ $[M + Na]^+$ 391.1050, found 391.1064.

4.1.6.4. 1-Phenyl-5-(4-(3-chlorophenyl)piperazine-1-carbonyl)-1H-tetrazol (6–4).

Light yellow Solid; yield: 58%; Mp: 102.5–104.0 °C; ^{1}H NMR (600 MHz, $CDCl_3$): δ = 7.58 (5H, m), 7.19 (1H, t, J = 8.1 Hz), 6.87 (2H, t, J = 8.5 Hz), 6.77 (1H, dd, J = 2.0 Hz, J = 8.1 Hz), 3.91 (2H, t, J = 5.0 Hz), 3.71 (2H, t, J = 5.0 Hz), 3.25 (2H, t, J = 4.8 Hz), 3.16 (2H, t, J = 5.4 Hz). ^{13}C NMR (150 MHz, $CDCl_3$): δ = 154.6, 150.5, 146.6, 134.1, 132.6, 129.7, 129.3, 128.8 (2 C), 123.0 (2 C), 119.7, 115.7, 113.7, 48.4, 47.8, 45.7, 41.3; HRMS calcd for $C_{18}H_{17}ClN_6NaO$ $[M + Na]^+$ 391.1050, found 391.1073.

4.1.6.5. 1-Phenyl-5-(4-(3-methylphenyl)piperazine-1-carbonyl)-1H-tetrazol (6–5).

White Solid; yield: 61%; Mp: 135.2–137.1 °C; ^{1}H NMR (600 MHz, $CDCl_3$): δ = 7.49 (5H, s), 7.10 (1H, s), 6.66 (3H, s), 3.85 (2H, s), 3.61 (2H, s), 3.15 (2H, s), 3.05 (2H, s), 2.25 (3H, s). ^{13}C NMR (150 MHz, $CDCl_3$): δ = 154.6, 149.5, 146.7, 138.1, 132.7, 129.7, 128.8 (2 C), 128.1, 122.9 (2 C), 120.9, 116.8, 113.0, 48.9, 48.5, 46.0, 41.5, 20.7; HRMS calcd for $C_{19}H_{20}N_6NaO$ $[M + Na]^+$ 371.1596, found 371.1633.

4.1.6.6. 1-Phenyl-5-(4-(3-methoxyphenyl)piperazine-1-carbonyl)-1H-tetrazol (6–6).

White Solid; yield: 67%; Mp: 144.3–146.2 °C; ^{1}H NMR (600 MHz, $CDCl_3$): δ = 7.57 (5H, d, J = 7.5 Hz), 7.20 (1H, t, J = 8.4 Hz), 6.50 (2H, m), 6.44 (1H, s), 3.92 (2H, t, J = 4.8 Hz), 3.7 (3H, s), 3.69 (2H, t, J = 5.1 Hz), 3.24 (2H, t, J = 4.9 Hz), 3.14 (2H, t, J = 4.8 Hz). ^{13}C NMR (150 MHz, $CDCl_3$): δ = 159.6, 154.6, 150.8, 146.6, 132.7, 129.7, 129.0, 128.8 (2 C), 123.0 (2 C), 108.5, 104.6, 102.4, 54.2, 48.8, 48.3, 45.9, 41.5; HRMS calcd for $C_{19}H_{20}N_6NaO_2$ $[M + Na]^+$ 387.1545, found 387.1578.

4.1.6.7. 1-Phenyl-5-(4-(4-methoxyphenyl)piperazine-1-carbonyl)-1H-tetrazol (6–7).

White Solid; yield: 71%; Mp: 152.7–154.2 °C; ^{1}H NMR (600 MHz, $CDCl_3$): δ = 7.51 (5H, m), 6.79 (4H, t, J = 13.5 Hz) , 3.86 (2H,s), 3.71 (3H, s), 3.62 (2H,s), 3.05 (2H, s), 2.95 (2H,s). ^{13}C NMR (150 MHz, $CDCl_3$): δ = 154.6, 153.7, 146.7, 143.7, 132.7, 129.6, 128.8 (2 C), 122.9 (2 C), 118.2 (2 C), 113.6 (2 C), 54.5, 50.3, 49.9, 46.1, 41.6; HRMS calcd for $C_{19}H_{20}N_6NaO_2$ $[M + Na]^+$ 387.1545, found 387.1574.

4.1.6.8. 1-Phenyl-5-(4-(3-trifluoromethyl)piperazine-1-carbonyl)-1H-tetrazol (6–8).

Light yellow Solid; yield: 60%; Mp: 77.7–79.2 °C; ^{1}H NMR (600 MHz, $CDCl_3$): δ = 7.59 (5H, m), 7.39 (1H, t, J = 7.8 Hz), 7.16 (1H, d, J = 7.8 Hz), 7.11 (1H, s), 7.06 (1H, d, J = 8.8 Hz), 3.95 (2H, t, J = 5.0 Hz), 3.76 (2H, t, J = 5.0 Hz), 3.30 (2H, t, J = 5.4 Hz), 3.22 (2H, t, J = 5.4 Hz). ^{13}C NMR (150 MHz, $CDCl_3$): δ = 154.6, 149.6, 146.5, 132.7, 129.7, 128.8, 128.8 (2 C), 128.7, 123.0 (2 C), 118.7, 116.3 (m), 114.2, 112.1 (m), 48.4, 47.9, 45.8, 41.4; HRMS calcd for $C_{19}H_{17}F_3N_6NaO$ $[M + Na]^+$ 425.1314, found 425.1311.

4.1.6.9. 1-Phenyl-5-(4-(3,4-dimethylphenyl)piperazine-1-carbonyl)-1H-tetrazol (6–9).

Pink Solid; yield: 57%; Mp: 138.6–140.1 °C; ^{1}H NMR (600 MHz, $CDCl_3$): δ = 7.57 (5H, m), 7.04 (1H, d, J = 8.1 Hz) , 6.73 (1H, s), 6.66 (1H, d, J = 8.4 Hz) , 3.29 (2H, t, J = 4.7 Hz), 3.68 (2H, s), 3.18 (2H, t, J = 5.4 Hz), 3.07 (2H, t, J = 4.7 Hz), 2.23 (3H, s), 2.19 (2H, s). ^{13}C NMR (150 MHz, $CDCl_3$): δ = 154.6, 147.6, 146.7, 136.5, 129.7, 129.3, 128.8 (2 C), 128.7, 122.9 (2 C), 117.9, 114.3, 113.6, 49.3, 49.0, 46.1, 41.6, 19.1, 17.8; HRMS calcd for $C_{20}H_{22}N_6NaO$ $[M + Na]^+$ 385.1753, found 385.1788.

4.1.6.10. 1-Phenyl-5-(4-(2,6-dimethylphenyl)piperazine-1-carbonyl)-1H-tetrazol (6–10).

Light yellow Solid; yield: 49%; Mp: 71.7–73.2 °C; ^{1}H NMR (600 MHz, $CDCl_3$): δ = 7.55 (5H, m), 7.08 (2H, d, J = 8.1 Hz), 6.83 (1H, t, J = 8.1 Hz), 3.74 (2H, s), 3.60 (2H, t, J = 4.0 Hz), 2.90 (2H, t, J = 5.4 Hz), 2.85 (2H, t, J = 4.7 Hz), 1.65 (6H, s). ^{13}C NMR (150 MHz, $CDCl_3$): δ = 169.2, 159.7, 150.7, 131.0, 130.7, 129.3 (2 C), 126.9 (2 C), 124.4 (2 C), 119.9 (2 C), 115.3, 52.0, 51.6, 46.9, 42.0, 17.4 (2 C); HRMS calcd for $C_{20}H_{22}N_6NaO$ $[M + Na]^+$ 385.1753, found 385.1788.

4.1.6.11. 1-Phenyl-5-(4-(3,4-dimethoxyphenyl)piperazine-1-carbonyl)-1H-tetrazol (6–11).

Light yellow Solid; yield: 53%; Mp: 101.6–102.6 °C; ^{1}H NMR (600 MHz, $CDCl_3$): δ = 7.59 (5H, d, J = 10.8 Hz), 7.80 (1H, d, J = 9.5 Hz), 6.55 (1H, s), 6.44 (1H, d, J = 8.1 Hz), 3.94 (2H, t, J = 6.1 Hz), 3.87 (3H, s), 3.84 (3H, s), 3.70 (2H, t, J = 5.4 Hz), 3.14 (2H, t, J = 5.1 Hz), 3.05 (2H, t, J = 5.5 Hz). ^{13}C NMR (150 MHz, $CDCl_3$): δ = 154.6, 148.5, 146.6, 144.2, 143.5, 132.7, 129.7, 128.8 (2 C), 122.9 (2 C), 110.7, 107.9, 102.6, 55.2, 54.8, 50.4, 50.1, 46.2, 41.7; HRMS calcd for $C_{20}H_{22}N_6NaO_3$ $[M + Na]^+$ 417.1651, found 417.1661.

4.1.6.12. 1-Phenyl-5-(4-(2,5-dimethoxyphenyl)piperazine-1-carbonyl)-1H-tetrazol (6–12).

Light yellow Solid; yield: 51%; Mp: 78.9–80.8 °C; ^{1}H NMR (600 MHz, $CDCl_3$): δ = 7.58 (5H, m), 6.79 (1H,

d, $J = 9.1$ Hz), 6.53 (1H, dd, $J = 2.5$ Hz, $J = 9.4$ Hz), 6.45 (1H, d, $J = 3.2$ Hz), 3.94 (2H, t, $J = 5.0$ Hz), 3.82 (3H, s), 3.76 (3H, s), 3.66 (2H, t, $J = 4.7$ Hz), 3.10 (2H, t, $J = 5.0$ Hz), 2.99 (2H, t, $J = 5.0$ Hz). ^{13}C NMR (150 MHz, $CDCl_3$): $\delta = 154.7$, 153.0, 146.8, 145.4, 139.9, 132.7, 129.6, 128.8 (2 C), 122.8 (2 C), 110.9, 105.6, 105.2, 54.8, 54.6, 49.7, 49.1, 46.3, 41.7; HRMS calcd for $C_{20}H_{22}N_6NaO_3$ $[M + Na]^+$ 417.1651, found 417.1693.

4.1.6.13. 1-Phenyl-5-(4-(3,5-dimethoxyphenyl)piperazine-1-carbonyl)-1H-tetrazol (6–13).

Light yellow Solid; yield: 61%; Mp: 121.3–123.2 °C; ^{1}H NMR (600 MHz, $CDCl_3$): $\delta = 7.57$ (5H, m), 6.07 (3H, m), 3.91 (2H, t, $J = 4.9$ Hz), 3.77 (6H, s), 3.69 (2H, t, $J = 4.7$ Hz), 3.23 (2H, t, $J = 4.9$ Hz), 3.13 (2H, t, $J = 5.0$ Hz). ^{13}C NMR (150 MHz, $CDCl_3$): $\delta = 160.5$ (2 C), 154.6, 151.3, 146.6, 132.6, 129.7, 128.8 (2 C), 122.9 (2 C), 94.8 (2 C), 91.6, 54.3 (2 C), 48.8, 48.3, 45.8, 41.4; HRMS calcd for $C_{20}H_{23}N_6O_3$ $[M + H]^+$ 395.1832, found 395.1859.

4.1.6.14. 1-(2-Fluorophenyl)-5-(4-(3-methylphenyl)piperazine-1-carbonyl)-1H-tetrazol (6–14).

Light yellow Solid; yield: 69%; Mp: 102.5–104.0 °C; ^{1}H NMR (600 MHz, $CDCl_3$): $\delta = 7.70$ (1H, m), 7.56 (1H, m), 7.39 (1H, t, $J = 8.1$ Hz), 7.28 (1H, t, $J = 9.5$ Hz), 7.19 (1H, t, $J = 8.1$ Hz), 6.77 (3H, t, $J = 6.7$ Hz), 4.03 (2H, t, $J = 4.7$ Hz), 3.92 (2H, t, $J = 4.7$ Hz), 3.27 (4H, t, $J = 5.1$ Hz), 2.34 (3H, s). ^{13}C NMR (150 MHz, $CDCl_3$): $\delta = 153.9$, 153.9 (d, $J = 245.7$ Hz), 149.6, 147.6, 131.3 (d, $J = 8.1$ Hz), 128.1, 125.9, 124.4 (d, $J = 3.5$ Hz), 123.1 (d, $J = 7.1$ Hz) 120.8, 116.7, 115.7 (d, $J = 19.4$ Hz), 114.7 (d, $J = 18.4$ Hz), 112.9, 48.9, 48.5, 46.2, 41.5, 20.7; HRMS calcd for $C_{19}H_{19}FN_6NaO$ $[M + Na]^+$ 389.1502, found 389.1531.

4.1.6.15. 1-(2-Fluorophenyl)-5-(4-(3-methoxyphenyl)piperazine-1-carbonyl)-1H-tetrazol (6–15).

Light yellow Solid; yield: 52%; Mp: 105.9–107.8 °C; ^{1}H NMR (600 MHz, $CDCl_3$): $\delta = 7.70$ (1H, m), 7.56 (1H, m), 7.38 (1H, t, $J = 7.6$ Hz), 7.28 (1H, t, $J = 9.8$ Hz), 7.21 (1H, t, $J = 8.7$ Hz), 6.56 (1H, m), 6.49 (2H, d, $J = 6.9$ Hz), 4.02 (2H, t, $J = 5.0$ Hz), 3.91 (2H, t, $J = 4.7$ Hz), 3.80 (3H, s), 3.28 (4H, t, $J = 5.0$ Hz). ^{13}C NMR (150 MHz, $CDCl_3$): $\delta = 159.6$, 153.9, 153.9 (d, $J = 251.7$ Hz), 150.9, 147.6, 131.4 (d, $J = 8.6$ Hz), 129.0, 125.9, 124.4 (d, $J = 3.8$ Hz), 121.3 (d, $J = 12.5$ Hz), 115.7 (d, $J = 18.1$ Hz), 108.5, 104.5, 102.3, 54.2, 48.7, 48.2, 46.1, 41.4; HRMS calcd for $C_{19}H_{19}FN_6NaO_2$ $[M + Na]^+$ 405.1451, found 405.1493.

4.1.6.16. 1-(2-Fluorophenyl)-5-(4-(3,5-dimethoxyphenyl)piperazine-1-carbonyl)-1H-tetrazol (6–16).

Yellow Solid; yield: 69%; Mp: 52.1–53.2 °C; ^{1}H NMR (600 MHz, $CDCl_3$): $\delta = 7.70$ (1H, m), 7.56 (1H, m), 7.39 (1H, t, $J = 7.8$ Hz), 7.29 (1H, m), 6.11 (2H, d, $J = 2.0$ Hz), 6.08 (1H, t, $J = 2.0$ Hz), 4.02 (2H, t, $J = 5.2$ Hz), 3.90 (2H, t, $J = 4.6$ Hz), 3.79 (6H, s), 3.27 (4H, t, $J = 5.2$ Hz). ^{13}C NMR (150 MHz, $CDCl_3$): $\delta = 160.6$ (2 C), 153.9, 153.9 (d, $J = 253.8$ Hz), 151.5, 147.6, 131.4 (d, $J = 7.6$ Hz), 126.0, 124.4 (d, $J = 3.5$ Hz), 121.3 (d, $J = 12.2$ Hz), 115.6 (d, $J = 19.3$ Hz), 94.8 (2 C), 91.5, 54.3 (2 C), 48.7, 48.2, 42.0, 41.4; HRMS calcd for $C_{20}H_{22}FN_6O_3$ $[M + H]^+$ 413.1737, found 413.1768.

4.1.6.17. 1-(3-Fluorophenyl)-5-(4-(3-methoxyphenyl)piperazine-1-carbonyl)-1H-tetrazol (6–17).

Light yellow Solid; yield: 64%; Mp: 124.3–126.0 °C; ^{1}H NMR (600 MHz, $CDCl_3$): $\delta = 7.54$ (1H, m), 7.40 (2H, t, $J = 8.1$ Hz), 7.28 (1H, t, $J = 8.8$ Hz), 7.20 (1H, t, $J = 9.4$ Hz), 6.53 (1H, d, $J = 8.3$ Hz), 6.49 (1H, d, $J = 7.6$ Hz), 6.45 (1H, s), 3.94 (2H, t, $J = 4.3$ Hz), 3.79 (3H, s), 3.76 (2H, t, $J = 5.0$ Hz), 3.27 (2H, t, $J = 5.8$ Hz), 3.20 (2H, t, $J = 4.7$ Hz). ^{13}C NMR (150 MHz, $CDCl_3$): $\delta = 161.7$ (d, $J = 245.2$ Hz), 159.6, 154.2, 150.7, 146.5, 133.7 (d, $J = 9.2$ Hz), 130.2 (d, $J = 8.6$ Hz), 129.1, 118.7 (d, $J = 3.0$ Hz), 116.8 (d, $J = 20.9$ Hz), 111.0 (d, $J = 27.5$ Hz),108.5, 104.7, 102.4, 54.2, 48.8, 48.3, 46.0, 41.6; HRMS calcd for $C_{19}H_{19}FN_6NaO_2$ $[M + Na]^+$ 405.1451, found 405.1500.

4.1.6.18. 1-(3-Fluorophenyl)-5-(4-(3,5-dimethoxyphenyl)piperazine-1-carbonyl)-1H-tetrazol (6–18).

Light yellow Solid; yield: 52%; Mp: 48.7–50.1 °C; ^{1}H NMR (600 MHz, $CDCl_3$): $\delta = 7.54$ (1H, m), 7.40 (2H, m), 7.28 (1H, m), 6.08 (3H, s), 3.94 (2H, t, $J = 5.3$ Hz), 3.78 (8H, s), 3.26 (2H, t, $J = 5.3$ Hz), 3.20 (2H, t, $J = 5.3$ Hz). ^{13}C NMR (150 MHz, $CDCl_3$): $\delta = 162.6$ (d, $J = 255.9$ Hz), 161.6 (2 C), 155.3, 152.3, 147.6, 134.8 (d, $J = 10.2$ Hz), 131.2 (d, $J = 9.6$ Hz), 119.8 (d, $J = 3.0$ Hz), 117.9 (d, $J = 20.8$ Hz), 112.1 (d, $J = 26.5$ Hz), 95.9 (2 C), 92.8, 55.3 (2 C), 49.9, 49.4, 46.9, 42.5; HRMS calcd for $C_{20}H_{22}FN_6O_3$ $[M + H]^+$ 413.1737, found 413.1759.

4.1.6.19. 1-(4-Fluorophenyl)-5-(4-(3-methoxyphenyl)piperazine-1-carbonyl)-1H-tetrazol (6–19).

White Solid; yield: 81%; Mp: 117.4–118.7 °C; ^{1}H NMR (600 MHz, $CDCl_3$): $\delta = 7.59$ (2H, m), 7.25 (2H, m), 7.19 (1H, t, $J = 8.4$ Hz), 6.52 (1H, dd, $J = 2.3$ Hz, $J = 8.4$ Hz), 6.48 (1H, dd, $J = 2.0$ Hz, $J = 8.4$ Hz), 6.45 (1H, s), 3.91 (2H, t, $J = 5.4$ Hz), 3.78 (5H, m), 3.25 (2H, t, $J = 5.4$ Hz), 3.20 (3H, t, $J = 5.0$ Hz). ^{13}C NMR (150 MHz, $CDCl_3$): $\delta = 163.5$ (d, $J = 245.7$ Hz), 160.7, 155.3, 151.8, 147.7, 130.1, 129.8 (d, $J = 2.5$ Hz), 126.5 (d, $J = 8.1$ Hz) (2 C), 116.9 (d, $J = 23.5$ Hz) (2 C), 109.5, 105.7, 103.4, 55.3, 49.9, 49.3, 47.1, 42.6; HRMS calcd for $C_{19}H_{19}FN_6NaO_2$ $[M + Na]^+$ 405.1451, found 405.1482.

4.1.6.20. 1-(4-Fluorophenyl)-5-(4-(3,5-dimethoxyphenyl)piperazine-1-carbonyl)-1H-tetrazol (6–20).

Brown Solid; yield: 45%; Mp: 48.1–49.4 °C; ^{1}H NMR (600 MHz, $CDCl_3$): $\delta = 7.59$ (2H, m), 7.25 (2H, m), 6.08 (3H, s), 3.91 (2H, t, $J = 4.7$ Hz), 3.78 (8H, s), 3.25 (2H, t, $J = 5.0$ Hz), 3.20 (2H, t, $J = 4.4$ Hz). ^{13}C NMR (150 MHz, $CDCl_3$): $\delta = 162.5$ (d, $J = 247.7$ Hz), 160.6 (2 C), 154.3, 151.3, 146.7, 128.8 (d, $J = 4.6$ Hz), 125.4 (d, $J = 9.2$ Hz) (2 C), 115.5 (d, $J = 23.5$ Hz) (2 C), 94.8 (2 C), 91.7, 54.3 (2 C), 48.9, 48.4, 45.9, 41.5; HRMS calcd for $C_{20}H_{22}FN_6O_3$ $[M + H]^+$ 413.1737, found 413.1774.

4.1.6.21. 1-(2-Chlorophenyl)-5-(4-(3-methylphenyl)piperazine-1-carbonyl)-1H-tetrazol (6–21).

Light yellow Solid; yield: 72%; Mp: 107.0–109.3 °C; ^{1}H NMR (600 MHz, $CDCl_3$): $\delta = 7.56$ (4H, m), 7.19 (1H, t, $J = 7.4$ Hz), 6.76 (3H, m), 4.09 (2H, t, $J = 4.75$ Hz), 3.87 (2H, t, $J = 5.4$ Hz), 3.27 (2H, t, $J = 5.4$ Hz), 3.24 (2H, t, $J = 5.4$ Hz), 2.33 (3H, s). ^{13}C NMR (150 MHz, $CDCl_3$): $\delta = 153.6$, 149.6, 148.0, 138.1, 131.1, 129.4, 129.4, 128.8, 128.1, 127.5, 127.1, 120.8, 116.7, 112.9, 48.9, 48.4, 46.2, 41.5, 20.7; HRMS calcd for $C_{19}H_{19}ClN_6NaO$ $[M + Na]^+$ 405.1207, found 405.1246.

4.1.6.22. 1-(2-Chlorophenyl)-5-(4-(3-methoxyphenyl)piperazine-1-carbonyl)-1H-tetrazol (6–22).

Light yellow Solid; yield: 74%; Mp: 99.8–101.5 °C; ^{1}H NMR (600 MHz, $CDCl_3$): $\delta = 7.56$ (4H, m), 7.21 (1H, t, $J = 9.1$ Hz), 6.55 (1H, dd, $J = 2.1$ Hz, $J = 8.4$ Hz), 6.48 (2H, m), 4.09 (2H, t, $J = 5.6$ Hz), 3.87 (2H, t, $J = 4.7$ Hz), 3.80 (3H, s), 3.29 (2H, t, $J = 5.2$ Hz), 3.25 (2H, t, $J = 4.7$ Hz). ^{13}C NMR (150 MHz, $CDCl_3$): $\delta = 159.6$, 153.6, 150.9, 148.0, 131.1, 131.0, 129.4, 129.0, 128.8, 127.5, 127.1, 108.4, 104.5, 102.3, 54.2, 48.8, 48.2, 46.1, 41.4; HRMS calcd for $C_{19}H_{19}ClN_6NaO_2$ $[M + Na]^+$ 421.1156, found 421.1199.

4.1.6.23. 1-(2-Chlorophenyl)-5-(4-(4-methoxyphenyl)piperazine-1-carbonyl)-1H-tetrazol (6–23).

Yellow Solid; yield: 68%; Mp: 119.9–121.2 °C; ^{1}H NMR (600 MHz, $CDCl_3$): $\delta = 7.56$ (4H, m), 6.92 (2H, d, $J = 8.8$ Hz), 6.86 (2H, d, $J = 9.5$ Hz), 4.08 (2H, t, $J = 4.7$ Hz),

3.87 (2H, t, $J = 4.7$ Hz), 3.78 (3H, s), 3.16 (2H, t, $J = 5.09$ Hz), 3.12 (2H, t, $J = 5.0$ Hz). ^{13}C NMR (150 MHz, $CDCl_3$): $\delta = 153.6$, 148.0 (2 C), 143.8, 131.1, 131.0, 129.4, 128.8, 127.5, 127.1, 118.1 (2 C), 113.5 (2 C), 54.5, 50.3, 49.7, 46.3, 41.6; HRMS calcd for $C_{19}H_{19}ClN_6NaO_2$ $[M + Na]^+$ 421.1156, found 421.1197.

4.1.6.24. 1-(2-Chlorophenyl)-5-(4-(3,4-dimethylphenyl)piperazine-1-carbonyl)-1H-tetrazol (6–24). Light yellow Solid; yield: 73%; Mp: 110.9–112.0 °C; ^{1}H NMR (600 MHz, $CDCl_3$): $\delta = 7.55$ (4H, m), 7.05 (1H, d, $J = 8.8$ Hz), 6.76 (1H, d, $J = 2.7$ Hz), 6.70 (1H, dd, $J = 2.7$ Hz, $J = 8.4$ Hz), 4.07 (2H, t, $J = 5.0$ Hz), 3.87 (2H, t, $J = 4.7$ Hz), 3.22 (2H, t, $J = 5.4$ Hz), 3.19 (2H, t, $J = 5.0$ Hz), 2.24 (3H, s), 2.19 (3H, s). ^{13}C NMR (150 MHz, $CDCl_3$): $\delta = 153.6$, 148.0, 147.8, 136.4, 131.1, 131.0, 129.4, 129.3, 128.8, 128.7, 127.5, 127.1, 117.8, 113.5, 49.4, 48.8, 46.2, 41.6, 19.2, 17.8; HRMS calcd for $C_{20}H_{21}ClN_6NaO$ $[M + Na]^+$ 419.1363, found 421.406.

4.1.6.25. 1-(2-Chlorophenyl)-5-(4-(3,5-dimethoxyphenyl)piperazine-1-carbonyl)-1H-tetrazol (6–25). Light yellow Solid; yield: 80%; Mp: 77.5–79.4 °C; ^{1}H NMR (600 MHz, $CDCl_3$): $\delta = 7.54$ (4H, m), 6.09 (2H, s), 6.08 (1H, s), 4.08 (2H, t, $J = 4.9$ Hz), 3.86 (2H, t, $J = 4.6$ Hz), 3.78 (6H, s), 3.27 (2H, t, $J = 4.6$ Hz), 3.24 (2H, t, $J = 5.5$ Hz). ^{13}C NMR (150 MHz, $CDCl_3$): $\delta = 161.6$ (2 C), 154.7, 152.5, 149.0, 132.2, 132.1, 130.4, 129.8, 128.5, 128.2, 95.8 (2 C), 92.6, 55.3 (2 C), 49.8, 49.2, 47.1, 42.5; HRMS calcd for $C_{20}H_{21}ClN_6NaO_3$ $[M + Na]^+$ 451.1261, found 451.1268.

4.1.6.26. 1-(3-Chlorophenyl)-5-(4-(3-methoxyphenyl)piperazine-1-carbonyl)-1H-tetrazol (6–26). White Solid; yield: 81%; Mp: 150.8–152.4 °C; ^{1}H NMR (600 MHz, $CDCl_3$): $\delta = 7.63$ (1H, s), 7.54 (1H, m), 7.50 (2H, d, $J = 4.7$ Hz), 7.20 (1H, t, $J = 8.9$ Hz), 6.53 (1H, d, $J = 8.4$ Hz), 6.49 (1H, d, $J = 9.5$ Hz), 6.45 (1H, s), 3.93 (2H, t, $J = 5.4$ Hz), 3.79 (5H, s), 3.27 (2H, t, $J = 5.0$ Hz), 3.21(2H, t, $J = 5.0$ Hz). ^{13}C NMR (150 MHz, $CDCl_3$): $\delta = 160.7$, 155.2, 151,8, 147.6, 135.6, 134.6, 130.9, 130.8, 130.1, 124.5, 122.3, 109.6, 105.7, 103.5, 55.3, 49.9, 49.4, 47.1, 42.6; HRMS calcd for $C_{19}H_{19}ClN_6NaO_2$ $[M + Na]^+$ 421.1156, found 421.1188.

4.1.6.27. 1-(3-Chlorophenyl)-5-(4-(3,5-dimethoxyphenyl)piperazine-1-carbonyl)-1H-tetrazol (6–27). Light yellow Solid; yield: 70%; Mp: 132.4–134.1 °C; ^{1}H NMR (600 MHz, $CDCl_3$): $\delta = 7.63$ (1H, s), 7.55 (1H, m), 7.50 (2H, m), 6.08 (3H, s), 3.93 (2H, t, $J = 5.2$ Hz), 3.78 (8H, s), 3.26 (2H, t, $J = 4.9$ Hz), 3.20 (2H, t, $J = 5.2$ Hz). ^{13}C NMR (150 MHz, $CDCl_3$): $\delta = 160.5$ (2 C), 154.1, 151.3, 146.6, 134.5, 133.6, 129.9, 129.7, 123.5, 121.3, 94.8 (2 C), 91.7, 54.3 (2 C), 48.9, 48.4, 45.9, 41.5; HRMS calcd for $C_{20}H_{22}ClN_6O_3$ $[M + H]^+$ 429.1442, found 429.1449.

4.1.6.28. 1-(2-Bromophenyl)-5-(4-(3,5-dimethoxyphenyl)piperazine-1-carbonyl)-1H-tetrazol (6–28). Yellow Solid; yield: 80%; Mp: 71.1–72.4 °C; ^{1}H NMR (600 MHz, $CDCl_3$): $\delta = 7.74$ (1H, dd, $J = 7.9$ Hz, $J = 1.0$ Hz), 7.56 (2H, m), 7.47 (1H, m), 6.09 (2H, s), 6.08 (1H, d, $J = 2.0$ Hz), 4.10 (2H, t, $J = 5.0$ Hz), 3.86 (2H, t, $J = 5.4$ Hz), 3.78 (6H, s), 3.29 (2H, t, $J = 5.0$ Hz), 3.24 (2H, t, $J = 5.4$ Hz). ^{13}C NMR (150 MHz, $CDCl_3$): $\delta = 160.5$ (2 C), 153.5, 151.5, 147.9, 132.6, 132.5, 131.4, 127.8, 127.7, 118.7, 94.7 (2 C), 91.5, 54.3 (2 C), 48.8, 48.1, 46.1, 41.4; HRMS calcd for $C_{20}H_{22}BrN_6O_3$ $[M + H]^+$ 473.0937, found 473.0954.

4.1.6.29. 1-(3-Bromophenyl)-5-(4-(3,5-dimethoxyphenyl)piperazine-1-carbonyl)-1H-tetrazol (6–29). White Solid; yield: 52%; Mp: 127.4–129.2 °C; ^{1}H NMR (600 MHz, $CDCl_3$): $\delta = 7.78$ (1H, t, $J = 1.8$ Hz), 7.70 (1H, d, $J = 8.3$ Hz), 7.54 (1H, d, $J = 7.9$ Hz), 7.44 (1H, t, $J = 8.3$ Hz), 6.09 (3H, s), 3.95 (2H, s), 3.78 (8H, s), 3.27 (2H, t, $J = 5.4$ Hz), 3.21 (2H, t, $J = 5.4$ Hz). ^{13}C NMR (150 MHz, $CDCl_3$): $\delta = 161.6$ (2 C), 155.1, 152.2, 147.6, 134.7, 133.8, 131.0, 129.7, 127.3, 122.8, 95.9 (2 C), 92.8, 55.3 (2 C), 50.0, 49.5, 47.0, 42.6; HRMS calcd for $C_{20}H_{21}BrN_6NaO_3$ $[M + Na]^+$ 495.0756, found 495.0784.

4.1.6.30. 1-(4-Bromophenyl)-5-(4-(3,5-dimethoxyphenyl)piperazine-1-carbonyl)-1H-tetrazol (6–30). Brown Solid; yield: 72%; Mp: 122.4–123.2 °C; ^{1}H NMR (600 MHz, $CDCl_3$): $\delta = 7.62$ (2H, d, $J = 8.6$ Hz), 7.40 (2H, d, $J = 8.6$ Hz), 6.01 (3H, s), 3.85 (2H, t, $J = 5.7$ Hz), 3.71 (8H, s), 3.19 (2H, t, $J = 5.3$ Hz), 3.14 (2H, t, $J = 5.2$ Hz). ^{13}C NMR (150 MHz, $CDCl_3$): $\delta = 160.5$ (2 C), 154.6, 152.1, 146.5, 131.9 (2 C), 131.6 (2 C), 124.7, 116.0, 94.9 (2 C), 91.2, 54.3 (2 C), 48.9, 48.4, 46.0, 41.6; HRMS calcd for $C_{20}H_{21}BrN_6NaO_3$ $[M + Na]^+$ 495.0756, found 495.0804.

4.1.6.31. 1-(2-Methylphenyl)-5-(4-(3,5-dimethoxyphenyl)piperazine-1-carbonyl)-1H-tetrazol (6–31). Yellow Solid; yield: 85%; Mp: 74.1–76.0 °C; ^{1}H NMR (600 MHz, $CDCl_3$): $\delta = 7.48$ (1H, t, $J = 7.6$ Hz), 7.40 (1H, d, $J = 7.8$ Hz), 7.36 (1H, t, $J = 7.4$ Hz), 7.26 (1H, s), 6.08 (3H, s), 3.95 (2H, t, $J = 5.7$ Hz), 3.83 (2H, t, $J = 5.0$ Hz), 3.77 (6H, s), 3.23 (2H, t, $J = 5.2$ Hz), 3.20 (2H, t, $J = 5.2$ Hz), 2.11 (3H, s). ^{13}C NMR (150 MHz, $CDCl_3$): $\delta = 160.5$ (2 C), 153.7, 151.4, 147.7, 133.8, 132.1, 130.4, 130.2, 125.9, 125.5, 94.8 (2 C), 91.6, 54.3 (2 C), 48.9, 48.3, 45.9, 41.4, 16.5; HRMS calcd for $C_{21}H_{24}N_6NaO_3$ $[M + Na]^+$ 431.1808, found 431.1849.

4.1.6.32. 1-(3-Methylphenyl)-5-(4-(3,5-dimethoxyphenyl)piperazine-1-carbonyl)-1H-tetrazol (6–32). Brown Solid; yield: 69%; Mp: 76.6–78.3 °C; ^{1}H NMR (600 MHz, $CDCl_3$): $\delta = 7.43$ (2H, m), 7.34 (2H, m), 6.09 (3H, s), 3.93 (2H, s), 3.78 (6H, s), 3.70 (2H, s), 3.24 (2H, t, $J = 5.4$ Hz), 3.15 (2H, s), 2.45 (3H, s). ^{13}C NMR (150 MHz, $CDCl_3$): $\delta = 160.6$ (2 C), 154.7, 151.2, 146.6, 139.2, 132.6, 130.5, 128.5, 123.5, 119.9, 95.0 (2 C), 91.9, 54.3 (2 C), 49.0, 48.5, 45.7, 41.3, 20.4; HRMS calcd for $C_{21}H_{24}N_6NaO_3$ $[M + Na]^+$ 431.1808, found 431.1854.

4.2. Biological evaluation

4.2.1. Cell culture

The human gastric adenocarcinoma SGC-7901 cells, lung adenocarcinoma A549 cells and cervical carcinoma HeLa cells were cultured in RPMI-1640 medium containing 10% FBS, 100 U/mL streptomycin and 100 U/mL penicillin at 37 °C in a humidified atmosphere containing 5% CO_2. All cell lines were purchased from the American Type Culture Collection (ATCC, Manassas, VA).

4.2.2. *In vitro* antiproliferative activity

The antiproliferative activity assay *in vitro* was carried out referring to the previously reported method[22].

4.2.3. Effect on tubulin polymerisation

The tubulin polymerisation assay was performed by using the commercial tubulin polymerisation assay kit (Cytoskeleton-Cat.#BK011P) referred to the protocol of manufacturer[23].

4.2.4. Analysis of immunofluorescence staining

Immunofluorescence staining studies were investigated using the reported method[24,25].

4.2.5. Cell cycle analysis

Cell cycle analysis assay was followed the procedure of relevant report[26].

4.3. Molecular modelling

Molecular modelling studies. Molecular docking was carried out by CDOCKER programme of Discovery Studio 3.0 software (PDB: 3HKC). The 3 D structure of 3HKC in docking study was downloaded from Protein Data Bank. The docking poses were selected according to previous studies[7].

Disclosure statement

No potential conflict of interest was reported by the author(s).

Funding

We gratefully acknowledge the National Natural Science Foundation of China [81673293 and 81602969], Project funded by China Postdoctoral Science Foundation [2018M641715], Liaoning Revitalisation Talents Programme [XLYC1802072] and Plan for Development of Young Scholars of Shenyang pharmaceutical university [ZQN2018002] for the generous financial support. This work was also supported by the Programme for Innovative Research Team of the Ministry of Education.

ORCID

Chao Wang http://orcid.org/0000-0002-1551-3592
Qi Guan http://orcid.org/0000-0002-5003-8723

References

1. Wang Q, Arnst KE, Wang Y, et al. Structure-guided design, synthesis, and biological evaluation of (2-(1H-indol-3-yl)-1H-imidazol-4-yl)(3,4,5-trimethoxyphenyl) methanone (ABI-231) analogues targeting the colchicine binding site in tubulin. J Med Chem 2019;62:6734–50.
2. Jiang L, Goto M, Zhu DQ, et al. Scaffold Hopping-driven optimization of 4-(quinazolin-4-yl)-3,4-dihydroquinoxalin-2(1H)-ones as novel tubulin inhibitors. ACS Med Chem Lett 2020;11:83–9.
3. Niu H, Strecker TE, Gerberich JL, et al. Design, structure guided design, synthesis, and biological evaluation of novel benzosuberene analogues as inhibitors of tubulin polymerization. J Med Chem 2019;62:5594–615.
4. Xu Q, Bao K, Sun M, et al. Design, synthesis and structure activity relationship of 3,6-diaryl-7H-[1,2,4]triazolo[3,4-b][1,3,4]thiadiazines as novel tubulin inhibitors. Sci Rep 2017;7:1–12.
5. Wasylyk C, Zheng H, Castell C, et al. Inhibition of the Ras-Net (Elk-3) pathway by a novel pyrazole that affects microtubules. Cancer Res 2008;68:1275–83.
6. Choi MJ, No ES, Thorat DA, et al. Synthesis and biological evaluation of aryloxazole derivatives as antimitotic and vascular-disrupting agents for cancer therapy. J Med Chem 2013;56:9008–18.
7. Wu Y, Feng D, Gao M, et al. Design and synthesis of 5-aryl-4-(4-arylpiperazine-1-carbonyl)-2*H*-1,2,3-triazole derivatives as colchicine binding site inhibitors. Sci Rep 2017;7:1–9.
8. Romagnoli R, Baraldi PG, Salvador MK, et al. Synthesis and evaluation of 1,5-disubstituted tetrazoles as rigid analogues of combretastatin A-4 with potent antiproliferative and antitumor activity. J Med Chem 2012;55:475–88.
9. Ibrahim YA, Al-Awadi NA, Al-Azemi TF, et al. Improved microwave synthesis of unsymmetrical N,N′-diaryl-1,2-aminoethane and imidazolidinium salts as precursors of N-heterocyclic carbenes. RSC Adv 2014;4:38869–76.
10. Pape F, Teichert JF. Tethered NHC ligands for stereoselective alkyne semihydrogenations. Synthesis 2017;49:2470–2482.
11. Fevig JM, Pinto DJ, Han Q, et al. Synthesis and SAR of benzamidine factor Xa inhibitors containing a vicinally-substituted heterocyclic core. Bioorg Med Chem Lett 2001;11:641–5.
12. Jia ZJ, Wu Y, Huang W, et al. 1-(2-Naphthyl)-1*H*-pyrazole-5-carboxylamides as potent factor Xa inhibitors. Part 3: design, synthesis and SAR of orally bioavailable benzamidine-P4 inhibitors. Bioorg Med Chem Lett 2004;14:1229–34.
13. Zhang X, Cai C, Winters M, et al. Design, synthesis and SAR of a novel series of heterocyclic phenylpropanoic acids as GPR120 agonists. Bioorg Med Chem Lett 2017;27:3272–8.
14. Quan ML, Ellis CD, He MY, et al. Nonbenzamidine tetrazole derivatives as factor Xa inhibitors. Bioorg Med Chem Lett 2003;13:369–73.
15. Chandrasekaran S, Ramanathan S, Basak T. Microwave material processing-a review. AIChE 2012;58:330–63.
16. Guan Q, Feng D, Bai Z, et al. Microwave-assisted synthesis, molecular docking and antiproliferative activity of (3/5-aryl-1,2,4-oxadiazole-5/3-yl)(3,4,5-trimethoxyphenyl)methanone oxime derivatives. MedChemComm 2015;6:1484–93.
17. Guan Q, Zuo D, Jiang N, et al. Microwave-assisted synthesis and biological evaluation of 3,4-diaryl maleic anhydride/*N*-substituted maleimide derivatives as combretastatin A-4 analogues. Bioorg Med Chem Lett 2015;25:631–4.
18. Wen Z, Xu J, Wang Z, et al. 3-(3,4,5-Trimethoxyphenylselenyl)-1*H*-indoles and their selenoxides as combretastatin A-4 analogs: microwave-assisted synthesis and biological evaluation. Eur J Med Chem 2015;90:184–94.
19. Hu H, Dong Y, Li M, et al. Design, synthesis and biological evaluation of novel thieno[3,2-d]pyrimidine and quinazoline derivatives as potent antitumor agents. Bioorg Chem 2019;90:1–11.
20. Juvale K, Wiese M. 4-substituted-2-phenylquinazolines as inhibitors of BCRP. Bioorg Med Chem Lett 2012;22:6766–9.
21. Paudel S, Acharya S, Yoon G, et al. Exploration of substituted arylpiperazine-tetrazoles as promising dual norepinephrine and dopamine reuptake inhibitors. Bioorg Med Chem 2016;24:5546–55.
22. Feng D, Wu Y, Wang H, et al. Synthesis and antiproliferative activity of 2-aryl-4-(3,4,5-trimethoxybenzoyl)-1,2,3-triazol derivatives as microtubule-destabilizing agents. RSC Advances 2017;7:29103–11.
23. Sun M, Xu Q, Xu J, et al. Synthesis and bioevaluation of *N*,4-diaryl-1,3-thiazole-2-amines as tubulin inhibitors with potent antiproliferative activity. PLoS One 2017;12:1–15.

24. Wang Z, Qi H, Shen Q, et al. 4,5-Diaryl-3*H*-1,2-dithiole-3-thiones and related compounds as combretastatin A-4/oltipraz hybrids: Synthesis, molecular modelling and evaluation as antiproliferative agents and inhibitors of tubulin. Eur J Med Chem 2016;122:520–9.
25. Wang Z, Yang Q, Bai Z, et al. Synthesis and biological evaluation of 2,3-diarylthiophene analogues of combretastatin A-4. Med Chem Commun 2015;6:971–6.
26. Xu Q, Sun M, Bai Z, et al. Design, synthesis and bioevaluation of antitubulin agents carrying diaryl-5,5-fused-heterocycle scaffold. Eur J Med Chem 2017;139:242–9.